Characterization and Drainage Kinetics of Colloidal Gas Aphrons

Divesh Bhatia, Gaurav Goel, Sidhartha K. Bhimania, and Ashok N. Bhaskarwar
Dept. of Chemical Engineering, Indian Institute of Technology, Delhi, Hauz Khas, New Delhi, 110 016, India

DOI 10.1002/aic.10552
Published online September 9, 2005 in Wiley InterScience (www.interscience.wiley.com).

The variation of air holdup and stability of colloidal gas aphrons (CGAs) with stirring time, surfactant concentration [6, 8.1, 10, and 12 mM sodium lauryl sulfate (SLS)], and stirring speed (3500–7000 rpm) was investigated, and an empirical correlation between the air holdup and stirring time was obtained. A first-order model for the drainage of CGAs was proposed and it correlated very well with the experimental data. A population balance model was proposed and correlated to the first-order drainage model to obtain an expression for the size distribution of CGA bubbles. A narrower size distribution at large stirring times was observed, which was correlated to the stability of CGAs. The stabilization of CGA dispersion with attainment of equilibrium size distribution at longer stirring times, analogous to homogenization of emulsions, was observed and an empirical expression for this time was reported. Mixing of two oppositely charged CGAs, generated using SLS (anionic) and cetyl trimethyl ammonium bromide (CTAB) (cationic), showed no effect on their stability, air holdup, and drainage kinetics. © 2005 American Institute of Chemical Engineers *AIChE J,* 51: 3048–3058, 2005
Keywords: colloidal gas aphrons, drainage kinetics, size distribution, oppositely charged CGAs, stability; air hold-up

Introduction

Sebba[1] first described colloidal gas aphrons (CGAs) as microfoam with colloidal properties. In a later study, Sebba[2] defined CGAs as microbubbles created by intense stirring (5000–10,000 rpm) of a surfactant solution. Characterization of CGAs—that is, the study of effects of various parameters, such as surfactant concentration, salt concentration, stirring time, pH, and temperature on air holdup and stability of CGAs—was done by Jauregi et al.[3] A review of the literature on CGAs was presented by Jauregi and Varley.[4] An updated summary of the literature on stability and drainage of CGAs is given in Table 1.

Correspondence concerning this article should be addressed to A. N. Bhaskarwar at ashoknb@chemical.iitd.ernet.in.

Theory

Structure and properties of CGAs

The term "colloidal" was used because of the small size of the bubbles (10–100 microns in diameter). Sebba[2] proposed that CGAs consisted of a gaseous inner core surrounded by a thin aqueous surfactant film composed of two surfactant layers and an outer electrical double layer that stabilized the structure, as shown in Figure 1. However, there is no real conclusive evidence available for this structure. CGAs are gas microbubbles and thus dynamic systems, continuously undergoing changes resulting from creaming, bubble breakage, coalescence, and disproportionation. Therefore, they possess a limited stability.

Some of the salient features of CGAs can be summarized as follows:

(1) Larger specific surface area and higher stability than those of normal bubbles because of their small size, like charges, and an electrical bilayer.

(2) Flow properties similar to those of water and a high gas

Table 1. Summary of the Open Literature on Stability and Drainage of CGAs

Author(s)	Surfactant*	Parameters Studied	Drainage Velocity	Bubble Size	Stability and Air Holdup	Conclusions
Jarudilokkul et al.[5]	Tween 20 (n)	Initial protein concentration, pH, protein/CGA volume ratio, surfactant concentration, rpm, stirring time, NaCl concentration			Yes	Stability increases with increasing surfactant concentration and stirring time. Separation decreases with increasing surfactant concentration. pH should be such that electrostatic interactions favor separation.
Jauregi et al.[6]	AOT (a)	pH, surfactant concentration, salt concentration, temperature	Yes	Yes	Yes	Aphron diameters could be predicted using models proposed for bubble breakage in agitated tanks and liquid drainage in foams and CGA dispersions. Drainage rate was predicted using foam drainage model modified for CGAs. Electron microscopy and X-ray diffraction techniques indicate the existence of an interface of many layers.
Jauregi and Varley[4]	AOT (a)	Stirring time, ionic strength, initial mass of protein, pH, protein/CGA volume ratio, magnetic stirrer speed			Yes	Speed of stirring and pH had little effect on separation parameters. Concentration of protein and surfactant in the initial mixture had an important effect on separation. The optimum protein recovery was 95% without significant loss of lysozyme activity.
Jauregi et al.[3]	AOT (a)	AOT concentration, temperature, stirring time, salt concentration, pH			Yes	Surfactant and salt concentration had maximum effect. Empirical equation for air holdup and half-life determined. Power required for generating CGAs decreases with increase in gas holdup.
Chaphalkar et al.[7]	HTAB (a) SDBS (c) Tergitol 15-S-12 (n)	Drainage time, type of surfactant, surfactant concentration, ionic strength		Yes	Yes	Bubble size in the range 30–300 μm. Mean diameter for Tergitol was reported to be less than that for SDBS and HTAB. Increase in surfactant concentration reduced the mean diameter for all three surfactants. Increase of ionic strength reduced mean diameter for ionic surfactants, but it had no effect on the nonionic surfactants.
Amiri et al.[8]	TTAB (c)		Yes		Yes	Drainage of CGAs was shown to be consistent with hindered rising of 35 μm spherical bubbles with 0.75 μm shells in downward flowing solution. The assumption of no coalescence may not hold good at later intervals. Ascertaining CGA dispersion—foam interface provides another limitation.

*n, nonionic surfactant; c, cationic surfactant; a, anionic surfactant.

content (55–65%), making them one of the lightest compressible liquids at ordinary temperature and pressure conditions.

(3) Hydrophobicity of the encapsulating surfactant shells, enabling them to collect oil globules, protein molecules, and so forth.

These features of CGAs provide applications such as the removal of naphthalene from a contaminated soil matrix,[9] separation of fine fibers from a lean slurry of cellulosic pulp in a flotation column,[10] and extraction of copper from aqueous acidic solution in LIX 622lkerosene (mixture of 5-dodecylsalicyal-dioxime and tridecanol in kerosene),[11] to cite but a few.

Characterization of CGAs

According to Sebba,[2] the formation of CGAs occurs as follows. The surface waves, generated as the result of intense stirring, strike against the baffles. They entrap a thin film of atmospheric air between the liquid and the surface of baffles, and reenter the solution. This film of air breaks into microbubbles or CGAs. Characterization of CGAs should involve considerations of the stability of the dispersion of microbubbles and the air holdup.

Stability. The stability of CGAs, measured in terms of half-life (t_{dh}), is defined as the time taken by "the CGAs dispersion–bulk liquid interface" to reach half its final height. The aphrons phase separates easily from the bulk-liquid phase because of its buoyancy. Figure 1 schematically shows the formation and drainage of CGAs as well as the state at half-life of CGAs.

Air Holdup. Air holdup is defined as the volume percentage of entrapped air in the CGA dispersion, expressed as

$$\varepsilon = \frac{(V_{To} - x')}{V_{To}} \times 100 \tag{1}$$

where V_{To} is the initial volume of CGA dispersion (m^3) and x' is the initial volume of surfactant solution (m^3).

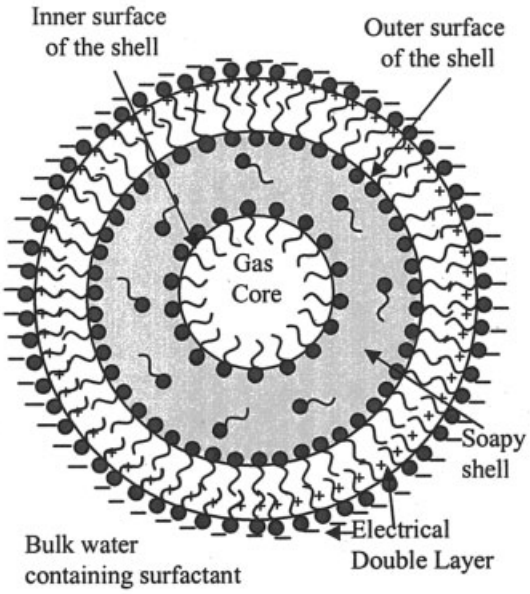

Proposed structure of CGAs [2]

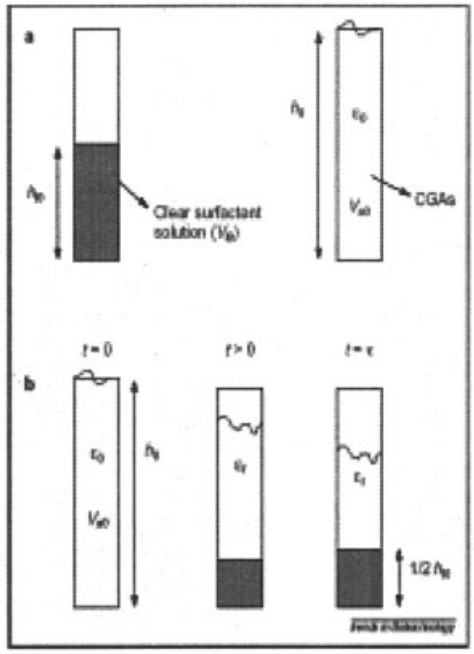

Schematic diagram showing (a) the formation and (b) the drainage of CGAs [12]

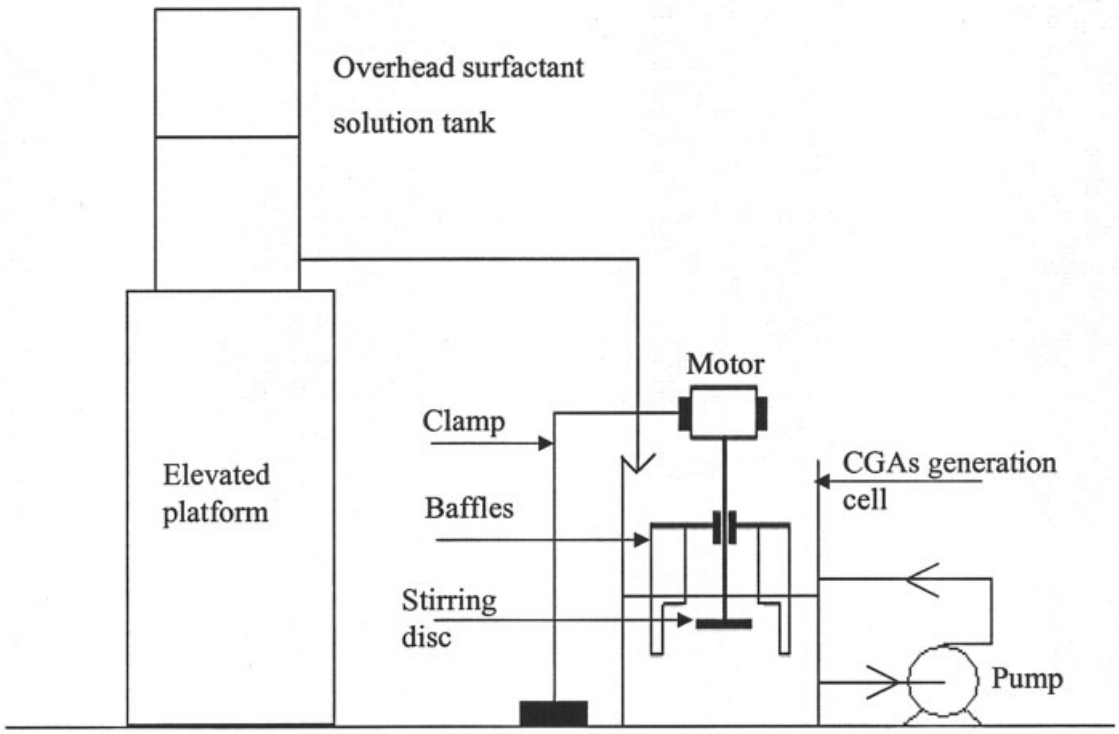

Experimental apparatus for CGAs generation

Figure 1. CGA diagrams.

Models for liquid drainage from CGAs

Model 1. The rate of drainage of liquid from CGAs is defined as

$$r = -\frac{dV_a}{dt_d} \tag{2}$$

where t_d is drainage time (s), and V_a is the volume of CGA dispersion at time t_d (m^3).

A first-order model is proposed for liquid drainage wherein the rate of drainage at a particular time is proportional to the volume of CGA dispersion still present at that time.

Thus, the first-order drainage equation is

$$-\frac{dV_a}{dt_d} = mV_a \tag{3}$$

where m is the rate constant for drainage (s^{-1}).

From the volume balance on CGA dispersion–bulk liquid system, assuming no air escapes from the system, we obtain

$$V_{To} = V_L + V_a \tag{4}$$

where V_L is the volume of surfactant solution in the bulk-liquid phase collected at the bottom at time t_d, (m^3).

By combining Eqs. 3 and 4, we obtain

$$\frac{d(V_{To} - V_L)}{dt_d} = -m(V_{To} - V_L) \tag{5}$$

The initial condition (a) for Eq. 5 is $V_L = 0$ at $t_d = 0$, and the solution of Eq. 5 subject to initial condition (a) is

$$\ln\left(\frac{V_{To} - V_L}{V_{To}}\right) = -mt_d \tag{6}$$

Model 2. Consistent with actual observations, a foam layer of constant thickness is assumed to be present at the top of the CGA dispersion. Because of buoyancy, CGAs rise to the aphron–foam interface, where they release most of the associated surfactant solution that drains down to enter the bulk-solution pool at the bottom. The following assumptions have been made while performing a population balance on the aphrons in the CGA dispersion:

(1) Aphrons are spherical and they are numerous enough to approximate their size distribution by a continuous function.

(2) Each aphron has an identical trajectory in the aphron-phase space.

(3) There is no breakage of aphrons.

(4) No new aphrons are formed in the system.

(5) The size of a particular aphron does not change with time.

A population balance for aphrons in a fixed subregion R_1 of the phase space is

$$\int_{R_1} [\partial n/\partial t_d + \nabla \cdot (v_x n) + \nabla \cdot (v_i n) + D - B]dR = 0$$

where n is the number of aphrons per unit length; v_x is the velocity of an aphron in the vertical direction; $v_i = dL/dt_d$, where L is the diameter of the aphron; D is the number of aphrons collapsing in unit time per unit length; and B is the number of aphrons forming in unit time per unit length.

Because the subregion R_1 is arbitrary, the integrand must vanish identically. D, B, and v_i are all equal to zero for our system because of the assumptions (3), (4), and (5), respectively. Thus, the population balance becomes

$$\frac{\partial n}{\partial t_d} + \frac{\partial (v_x n)}{\partial x} = 0 \tag{7}$$

where $n = n(x, t_d, L)$.

Suppose the aphrons are moving at their terminal velocity and Stokes law is applicable for individual aphrons of different sizes, even if in the presence of other sized aphrons. The velocity of the aphrons is

$$v_x(L) = \frac{gL^2\Delta\rho}{18\mu} = cL^2 \tag{8}$$

where $\Delta\rho$ is the difference between the densities of the aphrons and the surfactant solution and c ($=g\Delta\rho/18\mu$) is a constant for the system.

Substituting the value of $v_x(L)$ from Eq. 8 into Eq. 7, we obtain

$$\frac{\partial n}{\partial t_d} + c\frac{\partial (L^2 n)}{\partial x} = 0$$

It has been assumed that the diameter L does not vary with respect to time, and thus for rising aphrons with x. Thus,

$$\frac{\partial n}{\partial t_d} + cL^2\frac{\partial n}{\partial x} = 0 \tag{9}$$

Boundary conditions (b) and (c) for Eq. 9 are, respectively, $n(t_d = 0) = n_0$ and $n(x = 0) = 0$.

Solving Eq. 9 using Laplace transformation with boundary conditions (b) and (c), we obtain

$$n = n_0 \qquad 0 < t_d < \frac{x}{cL^2}$$

$$n = 0 \qquad t_d > \frac{x}{cL^2}$$

Let, at a particular time t_d, a bubble of diameter L' reach a height x. Equation 8 would then yield

$$L' = \sqrt{\frac{x}{ct_d}} \tag{10}$$

and the above solution becomes

$$n = n_0 \qquad 0 < L < L' \tag{11}$$

$$n = 0 \qquad L > L' \tag{12}$$

Consider an equivalent cylinder of diameter L_e and height L having the same volume as that of a spherical aphron of diameter L. Thus,

$$\frac{\pi L^3}{6} = \frac{\pi L_e^2}{4} L \tag{13}$$

That is, $L_e = (2/\sqrt{6})/L$.

The volume of aphrons of sizes between diameter L and $L + dL$ leaving the aphron–foam interface in time dt_d is given by

$$dV_G^L = -dt_d \left\{ \frac{v_x(L)\pi L_e^2}{4} n(H, t_d, L)dL \right\}$$

where H is the height of the aphron–foam interface.

Thus, the total volume of aphrons leaving the aphron–foam interface is

$$dV_G = -\left\{ \int_0^\infty \frac{v_x(L)\pi L_e^2}{4} n(H, t_d, L)dL \right\} dt_d$$

That is,

$$\frac{dV_G}{dt_d} = -\int_0^\infty \frac{v_x(L)\pi L_e^2}{4} n(H, t_d, L)dL$$

By inserting the values of $v_x(L)$ and L_e from Eqs. 8 and 13, respectively, we obtain

$$\frac{dV_G}{dt_d} = -\frac{\pi g \Delta\rho}{108\mu} \int_0^\infty L^4 n(H, t_d, L)dL$$

Recalling the values of n from Eqs. 11 and 12, we obtain

$$\frac{dV_G}{dt_d} = -\frac{\pi g \Delta\rho}{108\mu} \left[\int_0^{L'} L^4 n_0(L)dL + \int_{L'}^\infty L^4 n_0(L)dL \right] = -\frac{\pi g \Delta\rho}{108\mu} \int_0^{L'} L^4 n_0(L)dL \tag{14}$$

The volume of liquid drained is

$$V_L = V_{To}(1 - \varepsilon_0) - \frac{1 - \varepsilon}{\varepsilon} V_G \tag{15}$$

where ε_0 is the initial air holdup and V_G is the volume of gas in the CGA dispersion.

Equations 14 and 15, with the assumption of constant gas holdup with drainage time, yield

$$\frac{dV_L}{dt_d} = \frac{(1 - \varepsilon_0)\pi g \Delta\rho}{108\mu\varepsilon_0} \int_0^{L'} L^4 n_0(L)dL \tag{16}$$

For monodisperse aphrons in CGA dispersion (that is, $n_0(L) = n_0 =$ a constant), Eq. 14 leads to

$$\frac{dV_G}{dt_d} = -\frac{\pi g \Delta\rho n_0}{108\mu} \int_0^{L'} L^4 dL$$

and further, in view of Eqs. 8 and 10, we obtain

$$\frac{dV_G}{dt_d} = -\frac{n_0 \pi}{30} \left(\frac{H}{t_d}\right)^{5/2} \left(\frac{18\mu}{g\Delta\rho}\right)^{3/2}$$

Using Eq. 15 and the definition of c, we obtain

$$\frac{dV_L}{dt_d} = \frac{(1 - \varepsilon_0)n_0\pi}{30\varepsilon_0} \left(\frac{H}{t_d}\right)^{5/2} c^{-3/2} \tag{17}$$

Thus, Eq. 17 represents the liquid-drainage rate for a monodisperse CGA dispersion.

To obtain n_0 as a function of the aphron diameter, we equate the value of dV_L/dt_d from Eq. 6 to that from Eq. 16:

$$mV_{To}e^{-mt_d} = \frac{(1 - \varepsilon_0)\pi g \Delta\rho}{108\mu\varepsilon_0} \int_0^{L'} L^4 n_0(L)dL$$

that is,

$$\int_0^{\sqrt{H/ct_d}} L^4 n_0(L)dL = \frac{108\mu m V_{To}\varepsilon_0}{(1 - \varepsilon_0)\pi g \Delta\rho} e^{-mt_d}$$

It is assumed that $L^4 n_0(L)$ is a slowly varying function of time. Taking the derivative with respect to t_d, and substituting the value of t_d from Eq. 10, we obtain

$$n_0(L) = \frac{3888\mu^2 m^2 V_{To}\varepsilon_0 H}{(1 - \varepsilon_0)\pi g^2 (\Delta\rho)^2} \left(\frac{e^{-18m\mu H/g\Delta\rho L^2}}{L^7}\right) \tag{18}$$

Thus,

$$n_0(L) = \frac{a}{L^7} \exp\left(\frac{-b}{L^2}\right) \tag{19}$$

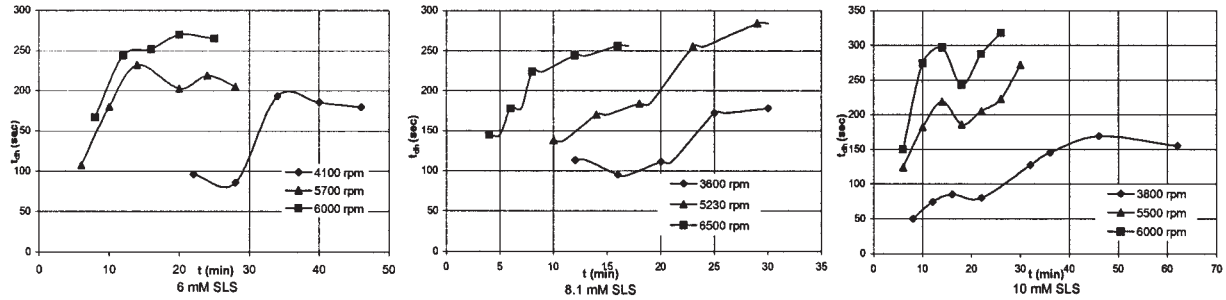

Figure 2. Half-life vs. stirring time for various SLS concentrations and stirring speeds.

where a and b are constants for a given system given by

$$a = \frac{3888\mu^2 m^2 V_{To}\varepsilon_0 H}{(1-\varepsilon_0)\pi g^2(\Delta\rho)^2} \tag{20}$$

$$b = \frac{18m\mu H}{g\Delta\rho} \tag{21}$$

By inserting the aphron-size distribution function $n_0(L)$ from Eq. 19 into Eq. 16, we obtain

$$\frac{dV_L}{dt_d} = \frac{(1-\varepsilon_0)}{\varepsilon_0}\frac{\pi ac}{12b}\, e^{-(bct_d/H)}$$

which leads to

$$V_L = \frac{(1-\varepsilon_0)}{\varepsilon_0}\frac{\pi aH}{12b^2}\,(1-e^{-(bct_d/H)}) \tag{22}$$

We therefore deduce the following equation:

$$\frac{dV_L}{dt_d} = \left(\frac{bc}{H}\right)\left[\frac{(1-\varepsilon_0)\pi aH}{12b^2\varepsilon_0} - V_L\right] \tag{23}$$

Thus, Eq. 23 predicts a first-order liquid-drainage rate for the CGAs with the aphron size distribution represented by Eq. 19.

Experimental Approach

The experimental setup consists of a 5-L beaker with two vertical inverted L-shaped baffles as shown in Figure 1. The surfactant solution is stirred in the beaker with a spinning disc at a constant stirring speed (>3000 rpm). The initial surfactant-solution level was 2 cm above the spinning disc.

To study the effects of parameters—surfactant concentration, stirring speed, and time of stirring—numerous sets of experiments were performed using surfactant concentrations below the critical micelle concentration (CMC) of SLS (6 mM), equal to the CMC (8.1 mM), and above the CMC (10 and 12 mM). One preliminary exploratory experiment was run for a long enough time such that there was no further change in the air holdup, that is, the steady state was achieved. Experiments were performed for various stirring speeds, ranging between 3000 and 7000 rpm. For the above sets of experiments performed, samples (~100 mL) of the stirred CGAs dispersions were taken out into measuring cylinders at different stirring-time intervals, and the rise of the (CGA-dispersion)–(bulk-liquid) interface with drainage time was noted.

In a separate set of experiments, CGAs were prepared from an anionic surfactant (8.1 mM SLS) and a cationic surfactant (2 mM CTAB) simultaneously, in two separate CGA generators. Methyl red dye was added to the SLS-based CGA generator, which provided a yellow color to the CGAs. Equal volumes (50 mL each) of the two oppositely charged CGAs were then stirred together on a magnetic stirrer for 30 s, and then poured into a 100-mL measuring cylinder. Simultaneously, 100-mL samples of SLS- and CTAB-based CGAs were separately charged to similar measuring cylinders, and the rise of the (CGA-dispersion)–(bulk-liquid) interface with drainage time was recorded for the three cases.

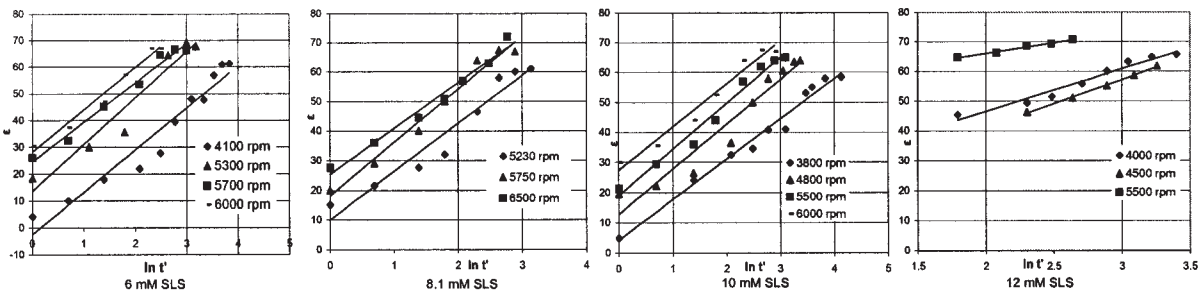

Figure 3. Air holdup vs. stirring time for various SLS concentrations and stirring speeds.

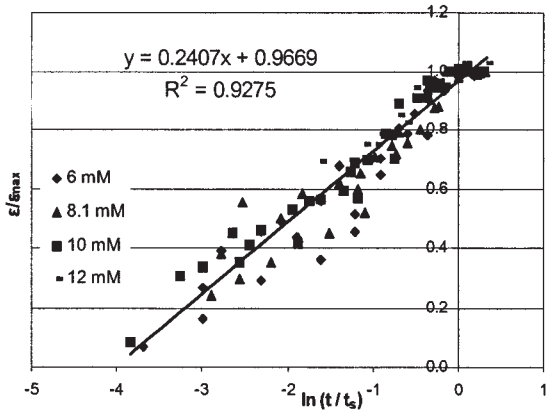

Figure 4. Best-fit line for air holdup fraction vs. ln(stirring time fraction).

Results and Discussion

Stability

Figure 2 shows the plots of half-life times vs. stirring time for different surfactant concentrations (sodium lauryl sulfate, 6–10 mM), each at three to four stirring speeds ranging from 3600 to 6500 rpm. For short stirring times, the (CGA-dispersion)–(bulk-liquid) interface was not clear, indicating a broad size distribution of aphrons. Data for such short times are therefore not being reported here. Figure 2 implies that the size distribution of aphrons improves with time, surfactant concentration, and stirring speed, seen in a general increase in the half-life time. The concentration range used by Jauregi et al.,[3] who reported an increase in half-life with concentration, was very large (0.1–34 mM for AOT). In contrast, the concentration range in the current experiments was much smaller (6–10 mM for SLS). As a result, there was only a limited increase in the half-life, that is, about 50–60 s. The increase in the stability of CGAs with surfactant concentration perhaps results from the increased repulsive forces between aphrons at higher concentrations of surfactant either in the surfactant shells or in the bulk-liquid phase.[13] Some of these experiments were run in duplicates and the average experimental error in measurements was estimated to be within ±7%.

Air holdup

Figure 3 shows the semilog plots of percentage air holdup vs. stirring time (nondimensionalized with unit time) for four different surfactant (sodium lauryl sulfate) concentrations (6, 8.1, 10, and 12 mM), and each at three to four stirring speeds (3800–6500 rpm). Figure 3 shows that as the time of stirring increases, the percentage air holdup increases irrespective of the surfactant concentration and stirring speed. This is because more air is entrapped with time into the system until the steady-state dispersion is reached. At low stirring speeds (<3000 rpm), there was no observable CGA formation. With an increase in stirring speed beyond 3000 rpm, for a fixed time of stirring and surfactant concentration, the air holdup increased, which can be attributed to the fact that with an increase in the stirring speed, the number of surface waves striking the baffles per unit time increased, thereby entrapping more air microbubbles in the CGA dispersion during the same time period.

Empirical correlation for air holdup

Figure 3 shows that for a given surfactant concentration, the semilog plots of air holdup vs. stirring time (nondimensionalized with unit time) are linear with almost equal slopes, and with increasing intercepts at higher stirring speeds. In an effort to bring all experimental data points onto a single curve, air holdup was scaled with the maximum air holdup (ε_{max}) for a particular stirring speed, and stirring time (t) was scaled with the time required to attain steady state (t_s). The data for four different surfactant concentrations (that is, 6, 8.1, 10, 12 mM SLS) mapped onto a single line of the form:

$$\varepsilon/\varepsilon_{max} = k \ln(t/t_s) + p \tag{24}$$

Figure 4 shows that the final air holdup correlation for the SLS–water system is

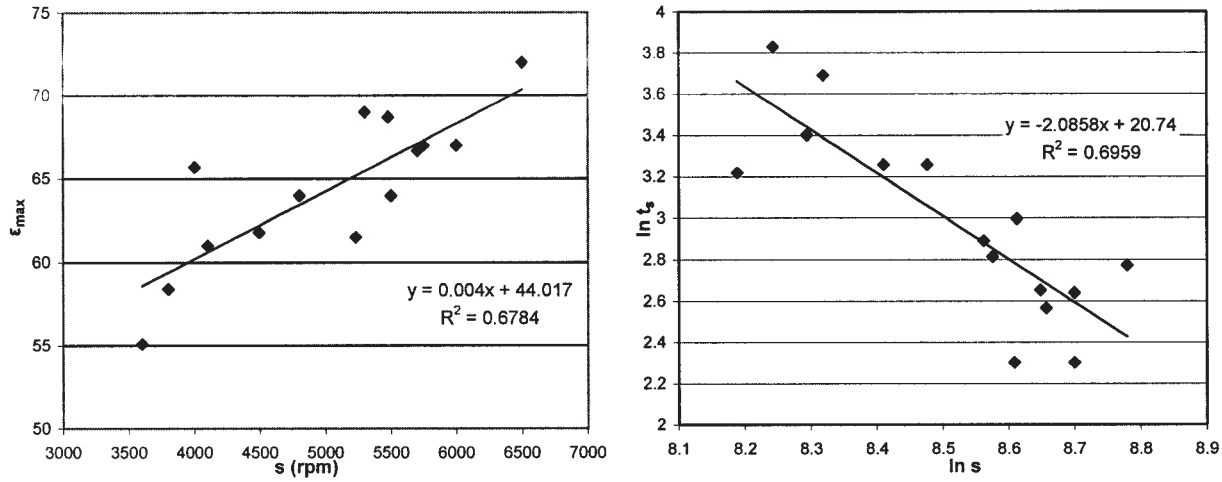

Figure 5. Variation of ε_{max} and t_s with stirring speed.

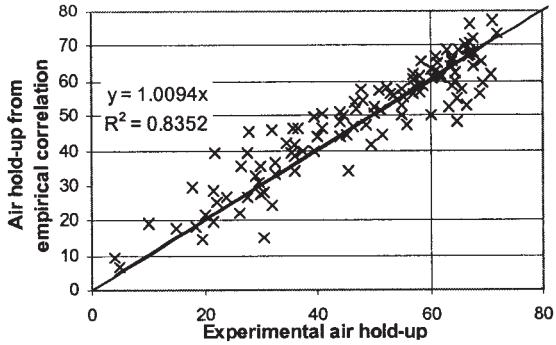

Figure 6. Comparison between experimental air holdup values and the values obtained from empirical correlation.

$$\varepsilon/\varepsilon_{\max} = 0.2407 \ln(t/t_s) + 0.9669 \quad (25)$$

with a correlation coefficient of $R^2 = 0.9275$.

This correlation has an implicit dependency of $\varepsilon_{\max}$ and t_s on the surfactant concentration and the stirring speed. Two out of the four surfactant concentrations used were above the CMC of SLS (8.1 mM), and one concentration was below the CMC. Figure 5 shows the variation of $\varepsilon_{\max}$ and t_s, respectively, with the stirring speed for all four surfactant concentrations. The corresponding R^2 values of 0.6784 and 0.6959 imply that the surfactant concentration, within the range used, does not have a significant effect on the air holdup. This observation is supported by Matsushita et al.,[14] who have reported no increase in air content for concentrations of CTMAB > 0.5 g L^{-1}. Interestingly, however, we find from our experiments for SLS that a concentration 25% lower than the CMC also leads to only a slight decrease in air holdup. The empirical dependency of $\varepsilon_{\max}$ and t_s on the stirring speed, as obtained from Figure 5, is

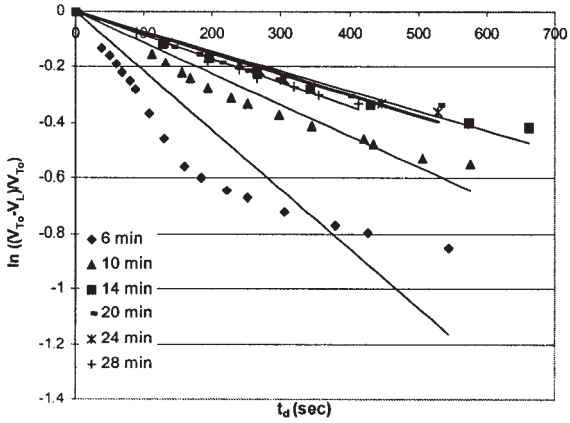

Figure 7. Plots of $\ln[(V_{To} - V_L)/V_{To}]$ vs. t_d at 6 mM SLS and 5700 rpm.

$$\varepsilon_{\max} = 0.004s + 44.017 \quad (26)$$

and

$$\ln t_s = -2.0858 \ln s + 20.74 \quad (27)$$

where s is stirring speed (rpm).

By combining Eqs. 25–27, we obtain the empirical dependency of air holdup on the stirring time and stirring speed as

$$\varepsilon = (0.004s + 44.017)\left(0.2407 \ln \frac{t}{s^{-2.0858}} - 4.025\right) \quad (28)$$

Figure 6 shows a comparison of the experimental values of air holdup with the calculated values from Eq. 28. An excellent

Table 2. Variation of Rate Constant with Stirring Speed and Stirring Time

6 mM				8.1 mM				10 mM			
Stirring Speed (rpm)	Stirring Time (min)	Negative of Slope (Eq. 6), m	Correlation Coefficient	Stirring Speed (rpm)	Stirring Time (min)	Negative of Slope (Eq. 6), m	Correlation Coefficient	Stirring Speed (rpm)	Stirring Time (min)	Negative of Slope (Eq. 6), m	Correlation Coefficient
5700	6	0.0021	0.72	3600	12	0.0032	0.99	4800	8	0.0026	0.48
	10	0.0011	0.91		16	0.0032	0.95		12	0.0012	0.63
	14	0.0007	0.95		20	0.0026	0.97		16	0.0009	0.68
	20	0.0007	0.92		25	0.0016	0.99		21	0.001	0.92
	24	0.0007	0.98		30	0.0015	0.96		26	0.0007	0.98
	28	0.0008	0.99		36	0.0012	1		29	0.0006	0.95
6000	8	0.0012	0.8	5230	10	0.002	1	5500	6	0.0015	0.54
	12	0.0007	0.94		14	0.0013	0.97		10	0.001	0.87
	16	0.0007	0.99		18	0.0012	0.99		14	0.0008	0.93
	20	0.0006	0.98		23	0.0009	0.99		18	0.0007	0.83
	25	0.0007	0.99		29	0.0008	0.99		22	0.0007	0.86
					35	0.0008	0.99		26	0.0007	0.98
				5750	6	0.0014	0.98		30	0.0007	0.99
					10	0.0007	1	6000	6	0.0013	0.8
					14	0.0006	0.99		10	0.0007	1
					18	0.0007	1		14	0.0006	1
				6500	6	0.0015	0.98		18	0.0007	0.97
					8	0.0011	0.97		22	0.0006	0.99
					12	0.0008	1		26	0.0006	1
					16	0.0013	0.54				

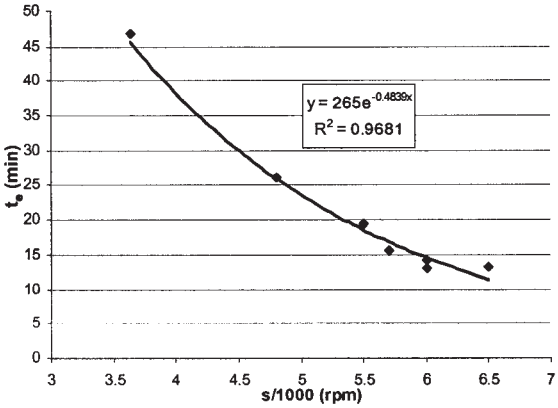

Figure 8. Equilibrium time vs. stirring speed.

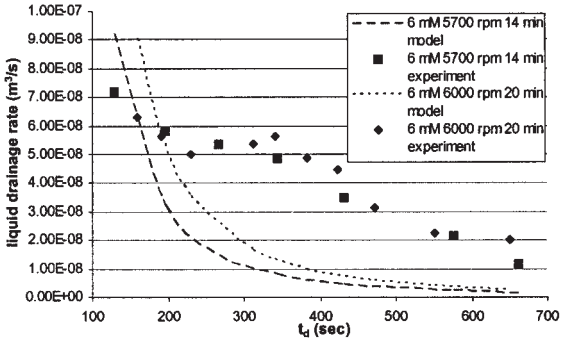

Figure 10. Comparison of experimental and model-predicted liquid drainage rate.

agreement between the two sets of values ($R^2 = 0.8352$) implies that Eq. 28 can express the experimental results very well within the surfactant (SLS) concentration range explored.

Liquid drainage from CGAs

There was a rise in the (CGA-dispersion)–(bulk-liquid) interface with time as a result of the creaming, coalescence of CGAs, and the accompanying liquid drainage. Figure 7 shows the plots of $\ln[(V_{To} - V_L)/V_{To}]$ vs. t_d, for 6 mM SLS and for different stirring times at a speed of 5700 rpm. The plots for various other stirring speeds and surfactant concentrations were similar and are summarized in Table 2 in terms of the slopes and correlation coefficients. The high correlation-coefficient values show that the experimental data correlated well with the first-order drainage kinetics represented by Eq. 6. The values of the drainage-rate constant varied from 0.0032 to 0.0006, decreasing with increasing stirring speeds and stirring times, as shown in Table 2. This indicates an increase in the stability of CGA dispersion, which can be attributed to the attainment of a narrower size distribution of CGAs in the dispersion. The convergence of m values to a constant value of 0.0007 with increasing stirring times indicates that an equilibrium size distribution will be attained for all stirring speeds above the critical stirring speed for CGA generation. However, the time required to attain this equilibrium size distribution, t_e, will be larger for lower stirring speeds. It decreases exponentially with stirring speed as shown in Figure 8. The stirring time was scaled with t_e, and the drainage-rate constant m was plotted against this nondimensional stirring time. A fourth-degree polynomial fit was used for these data as shown in Figure 9.

The best-fit values of n_0 were obtained by fitting the experimental liquid-drainage rates to Eq. 17 for various values of surfactant concentrations, stirring times, and stirring speeds. Figure 10 shows a comparison of the experimental values of drainage rates with the predicted values from Eq. 17. Figure 10 also shows that the model predicts a faster decrease in drainage rate with time in contrast to the experimental data. The comparisons for other stirring speeds, surfactant concentrations, and stirring times yielded similar trends.

The experimentally measured surfactant-solution volume was next used in Eq. 22 to find the best-fit values of a and b for various values of surfactant concentrations, stirring times, and stirring speeds. These were further used to calculate $n_0(L)$ from Eq. 19. Figure 11 shows the variation of n_0 with the aphron diameter for 6 mM SLS and different stirring times at a speed of 5700 rpm. Figure 11 also shows that the size distribution of aphrons becomes narrower with increasing stirring time, further consolidating the analogous notion of homogenization. The variation of $n_0(L)$ for various other stirring speeds and surfactant concentrations yielded similar results. The increase of stability with stirring time can thus be explained by a narrower size distribution of aphrons at longer stirring times. At short stirring times, the size distribution is broad, leading to

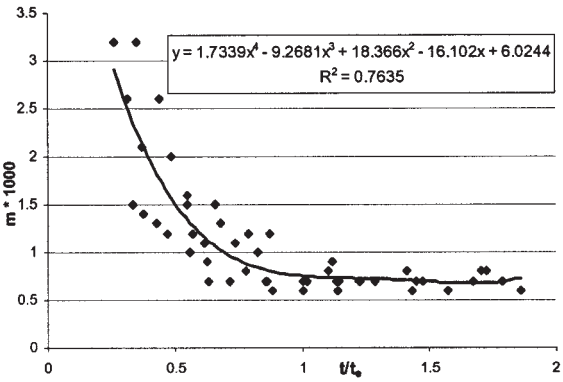

Figure 9. Plot of *m* vs. nondimensional stirring time for various stirring speeds.

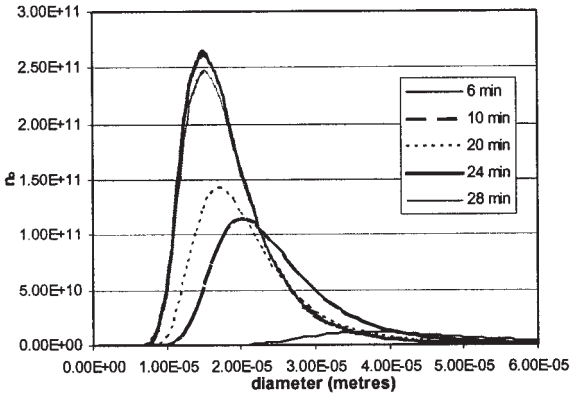

Figure 11. Aphron size distribution for 6 mM, 5700 rpm, and various stirring times.

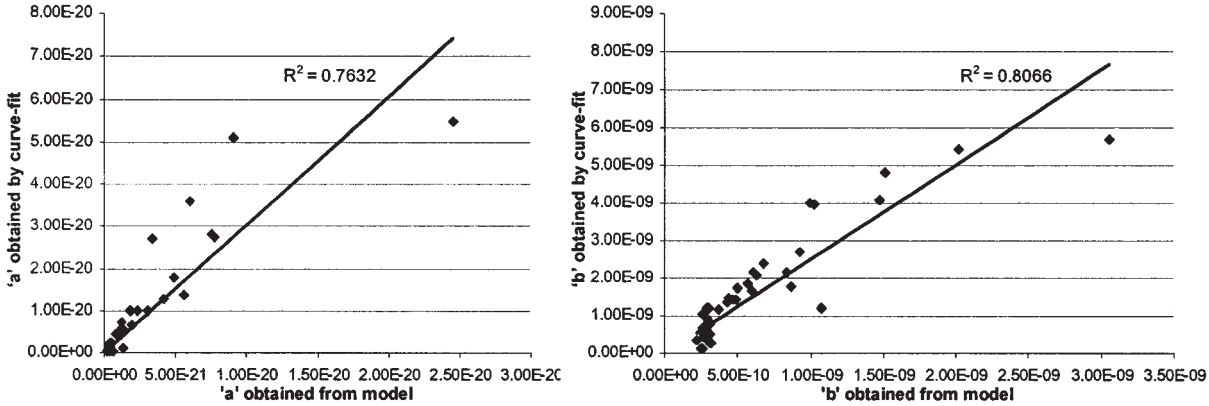

Figure 12. Comparison between parameters *a* and *b* obtained by curve fitting and model.

a hazy interface between dispersion of CGAs and the bulk surfactant solution.

The values of a and b obtained by fitting the experimental data to Eq. 22 were compared with the values calculated using Eqs. 20 and 21. Figure 12 shows that the values of a and b obtained using Eqs. 20 and 21 are in agreement with those obtained by fitting the experimental data to Eq. 22 to within an order of magnitude. The size distribution of aphrons, represented by Eq. 19, can therefore broadly explain the first-order drainage kinetics of CGAs represented by Eq. 23.

Mixing of oppositely charged CGAs

Visual Observation. A 50-mL solution of SLS-based CGAs, colored yellow with methyl red dye, was charged to a 100-mL measuring cylinder. A CTAB-based solution of CGAs (50 mL) was then slowly added to the cylinder. It was observed that the whole dispersion turned lighter yellow, as a result of dilution, indicating the mixing of the oppositely charged CGAs.

Drainage-Rate Measurements. Figure 13 shows $\ln[(V_{To} - V_L)/V_{To}]$ vs. t_d plots for the drainage data obtained from experiments similar to those described earlier.

The following observations may be made:

(1) The drainage curves overlap, indicating practically no change in the drainage kinetics on mixing of the oppositely charged CGAs, in contrast to oppositely charged foams that are known to quickly destroy each other.[2]

(2) Upon mixing of oppositely charged CGAs, no appreciable changes in stability and air holdup are observed, as seen in Table 3.

(3) The foam formed above the mixed (oppositely charged) CGAs, however, collapsed much faster than that above the dispersions of individual CGAs, indicating the instability of foam resulting from the oppositely charged surfactants. This feature may be useful in quickly destroying the creamed foam formed in applications of CGAs, such as for separation of oils, pigments/dyes, and proteins, from aqueous emulsions, dispersions, or solutions.

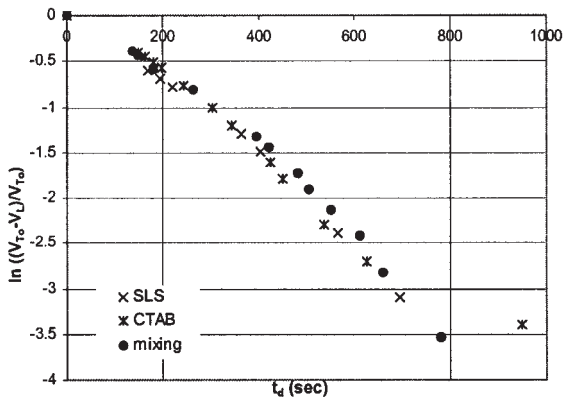

Figure 13. Plot of $\ln[(V_{To} - V_L)/V_{To}]$ vs. drainage time for SLS, CTAB, and their mixture.

Conclusions

Characterization of CGAs has been done, and an empirical correlation for the variation of air holdup with stirring time and stirring speed has been developed. First-order kinetics for drainage of CGAs has been proposed and the resultant expression was validated experimentally. A new population balance model has been developed, which for the first-order drainage kinetics yielded an expression for the size distribution of aphrons. This size distribution has been used to explain the effect of stirring time on the stability of CGAs. Convergence of the drainage-rate constant values indicates that an equilibrium size distribution of aphrons for the dispersion is attained at a finite time t_e for all stirring speeds above the critical speed for formation of CGAs. An empirical correlation for t_e was found to be an exponentially decreasing function of the stirring speed. For the first time, the behavior upon mixing of two oppositely charged CGAs has been studied and the results surprisingly show no effect on drainage and stability, except in the tail-end foam stage.

Table 3. Effect of Mixing of Oppositely Charged CGAs on Stability and Air Holdup

	Air Holdup (%)	Half-life (s)
SLS	59.25	194
CTAB	65.9	229
Mixture	64.23	223

Notation

B = number of aphrons forming in unit time per unit length, $s^{-1}\ m^{-1}$
dV_G = volume of aphrons leaving the aphron–foam interface in time dt_d, m^3
dV_G^L = volume of aphrons between diameter L and $L + dL$ leaving the aphron–foam interface in time dt_d, m^3
D = number of aphrons collapsing in unit time per unit length, $s^{-1}\ m^{-1}$
H = height of the aphron–foam interface, m
L = diameter of the aphron, m
L_e = diameter of cylinder of height L and having the same volume as a sphere of diameter L, m
m = rate-constant for drainage, s^{-1}
n = number of aphrons per unit length, m^{-1}
n_0 = number of aphrons per unit length at $t_d = 0$, m^{-1}
r = rate of drainage of liquid from CGAs, $m^3\ s^{-1}$
s = stirring speed, rpm
t = stirring time, min
t_d = drainage time, s
t_{dh} = half-life of CGAs, s
t_e = time required for attaining equilibrium size distribution, min
t_s = time required for attaining steady state for a given stirring speed, min
t' = nondimensionalized stirring time [$=t/(1\ min)$], dimensionless
v_x = velocity of an aphron in the vertical direction, ms^{-1}
V_a = volume of CGA dispersion at time t_d, m^3
V_G = volume of gas in the CGA dispersion at time t_d, m^3
V_L = volume of surfactant solution in bulk-liquid phase collected at the bottom at time t_d, m^3
V_{To} = total initial volume of CGA dispersion, m^3
x = vertical coordinate, m
x' = initial volume of surfactant solution, m^3
ε = percentage air holdup of CGAs, dimensionless
ε_{max} = maximum air holdup for a given stirring speed, dimensionless
ε_0 = percentage air holdup of CGAs at $t_d = 0$, dimensionless
$\Delta\rho$ = difference in densities of the aphrons and the surfactant solution, kg/m^3

Literature Cited

1. Sebba F. Microfoams—An unexploited colloid system. *J Colloid Interface Sci.* 1971;35:643-646.
2. Sebba F. *Foams and Biliquid Foams: Aphrons*. 1st Edition. Chichester, UK: Wiley; 1987.
3. Jauregi P, Gilmour S, Varley J. Characterisation of colloidal gas aphrons for subsequent use for protein recovery. *Chem Eng J.* 1997; 65:1-11.
4. Jauregi P, Varley J. Colloidal gas aphrons: A novel approach to protein recovery. *Biotechnol Bioeng.* 1998;59:471-481.
5. Jarudilokkul S, Rungphetcharat K, Boonamnuayvitaya V. Protein separation by colloidal gas aphrons using nonionic surfactant. *Sep Purif Technol.* 2004;35:23-29.
6. Jauregi P, Mitchell GR, Varley J. Colloidal gas aphrons (CGA): Dispersion and structural features. *AIChE J.* 2000;46:24-36.
7. Chaphalkar PG, Valsaraj KT, Roy D. A study of the size distribution and stability of colloidal gas aphrons using a particle size analyzer. *Sep Sci Technol.* 1993;28:1287-1302.
8. Amiri MC, Woodburn ET. A method for the characterization of colloidal gas aphron dispersions. *Trans IChemE.* 1990;68A:154-160.
9. Roy D, Kongara S, Valsaraj KT. Applications of surfactant solutions and colloidal gas aphron suspensions in flushing naphthalene from a contaminated soil matrix. *J Hazard Mater.* 1995;42:247-263.
10. Hashim MA, Gupta BS. The application of colloidal gas aphrons in the recovery of fine cellulose fibres from paper mill wastewater. *Bioresource Technol.* 1998;64:199-204.
11. Save SV, Pangarkar VG, Kumar SV. Liquid–liquid extraction using aphrons. *Sep Technol.* 1994;4:104-111.
12. Jauregi P, Varley J. Colloidal gas aphrons: Potential applications in biotechnology. *Trends Biotechnol.* 1999;17:389-395.
13. Noble M, Brown A, Jauregi P, Kaul A, Varley J. Protein recovery using gas–liquid dispersions. *J Chromatogr B Biomed Sci Appl.* 1998; 711:31-43.
14. Matsushita K, Mollah AH, Stuckey DC, Cerro CD, Bailey AI. Predispersed solvent extraction of dilute products using colloidal gas aphrons and colloidal liquid aphrons: Aphron preparation, stability and size. *Colloids Surf.* 1992;69:65-72.

Manuscript received Apr. 6, 2004, and revision received Mar. 4, 2005.